Palaeogeography, Palaeoclimatology, Palaeoecology 297 (2010) 214–222

Contents lists available at ScienceDirect

Palaeogeography, Palaeoclimatology, Palaeoecology

journal homepage: www.elsevier.com/locate/palaeo

Anti-phase oscillation of Asian monsoons during the Younger Dryas period: Evidence from peat cellulose $\delta^{13}C$ of Hani, Northeast China

B. Hong [a,*], Y.T. Hong [a], Q.H. Lin [a], Yasuyuki Shibata [b], Masao Uchida [b], Y.X. Zhu [a], X.T. Leng [c], Y. Wang [a], C.C. Cai [a]

[a] State Key Laboratory of Environmental Geochemistry, Institute of Geochemistry, Chinese Academy of Sciences, 46 Guanshui Road, Guiyang, Guizhou 550002, China
[b] Environmental Chemistry Division, National Institute for Environmental Studies, Onogawa 16-2, Tsukuba, Ibaraki, 305-0053, Japan
[c] Institute of Peatmire, Northeast Normal University, Changchun, Jilin 130024, China

ARTICLE INFO

Article history:
Received 4 March 2010
Received in revised form 6 August 2010
Accepted 8 August 2010
Available online 13 August 2010

Keywords:
Younger Dryas
East Asian monsoon
Indian Ocean monsoon
Paleo-El Niño
Western Pacific subtropical high
Peat cellulose isotope

ABSTRACT

Significant changes in the global atmospheric and oceanic circulation system occurred during the Younger Dryas cold period. Several researchers have demonstrated a weakening of intensity of the Indian Ocean Summer Monsoon during that period. However, the exact characteristics of the East Asian Summer Monsoon still remain vague. Here we present a late-glacial precipitation proxy record of the East Asian Summer Monsoon, based on the peat cellulose $\delta^{13}C$ found in Hani, Northeast China. Both the peat cellulose record and a pollen record from Lake Sihailongwan sediment indicate an abrupt increase in precipitation in the region during the Younger Dryas period. These results support the occurrence of wet conditions in the north and of dry conditions in the south of the Chinese Mainland during that period. By examining the activity of the East Asian Summer Monsoon on an interannual timescale, we propose a theory for the anomalous precipitation distribution that we attribute to the occurrence of an El Niño-like phenomenon in the Equatorial Pacific Ocean during the Younger Dryas. In this case, the intensity of the Western Pacific subtropical high may strengthen, and its position over the western Pacific Ocean may move northward. This could cause an enhancement of the East Asian Summer Monsoon and migration of a monsoonal rainbelt towards the northern region of the Chinese mainland, resulting in a precipitation distribution of wet conditions in the north and dry conditions in the south. Therefore, this anomalous rainfall distribution should be considered to indicate the strengthening of the East Asian Summer Monsoon, in anti-phase with the Indian Ocean Summer monsoon that weakened during the same period. This agrees with the previously revealed anti-phase variations of the two monsoons during the ice-rafted debris cold events of the North Atlantic Ocean. It appears that, in relation to the abrupt temperature drop in the Northern Hemisphere on centennial to millennial time scales, anti-phase variations of the two Asian summer monsoons occurred.

1. Introduction

During the Younger Dryas (YD) cold period, the global atmospheric and oceanic circulation patterns reorganized, and a series of abrupt climatic changes on centennial to millennial time scales appeared. Geological archives have revealed that since around 13 000 cal.yr BP, freshwater pulses have extended into the high-latitude North Atlantic Ocean on several occasions (Teller et al., 2002). Also, the meridional overturning circulation that crosses the equator slowed down (Rooth, 1982; Broecker et al., 1985; Knutti et al., 2004). The temperature of both the oceanic surface water and the atmosphere of the North Atlantic Ocean region decreased, and a large part of the Northern Hemisphere cooled (Bond et al., 1997; Alley, 2000; Hong et al., 2009). Meanwhile, the sea surface temperature (SST) of the middle-east equatorial Pacific Ocean tended to warm, the gradient of the SST in the equatorial Pacific Ocean decreased, and the El Niño-like pattern phenomenon appeared (Koutavas et al., 2002). During the same interval, the intensity of the Indian Ocean Summer Monsoon (IOSM) underwent an obvious abrupt weakening (Gasse et al., 1991; Roberts et al., 1993; Sirocko et al., 1996; Schulz et al., 1998). This phenomenon of global teleconnection provides a unique foundation for investigating changes in the Earth system. Several hypotheses or considerations related to the forcing mechanism for climate changes during the YD period have been presented. Examples are the hypothesis on the variation of ocean thermohaline circulation (THC) in the Northern high latitudes; the hypothesis on the driving of the ocean–atmosphere interaction in low latitudes; the variation of solar activity and the movements of the Intertropical Convergence Zone (ITCZ); and the combined effect of solar activity, THC, ENSO, and other phenomena (Bond et al., 2001; Broecker, 2003; Clement and Peterson, 2008; Hong et al., 2009).

* Corresponding author. Tel.: +86 851 5891248; fax: +86 851 5891609.
E-mail address: hongbing@vip.skleg.cn (B. Hong).

0031-0182/$ – see front matter © 2010 Elsevier B.V. All rights reserved.
doi:10.1016/j.palaeo.2010.08.004

However, against this background of global changes, available knowledge of the East Asian Summer Monsoon (EASM) during the YD is still quite vague. Research studies examining lake sediments and loess paleosol have suggested an abrupt strengthening of the EASM during the YD interval (Kelts et al., 1989; An et al., 1993; Wang et al., 1994; Zhou et al., 1996), which means changes in the EASM and IOSM had an anti-phase relationship during this period. Conversely, other research based on marine sediments and stalagmite isotopes have indicated an abrupt weakening of the EASM during the YD, which indicates an in-phase relationship between the EASM and IOSM (Wang et al., 1999; Wang et al., 2001; Yuan et al., 2004; Huang et al., 2009). These contradictory results have aroused the concern of paleoclimate scholars. To better understand the teleconnections and the mechanism hypotheses mentioned earlier, it is essential to better clarify how the EASM strength varies, as this understanding is a weak link in global climatic change research on the YD interval.

Here, we present a high-resolution and sensitive proxy record of EASM monsoonal precipitation using Hani peat cellulose $\delta^{13}C$ from Northeast China. By comparing this proxy record with the pollen record from the sediments of Lake Sihailongwan near the Hani peat mire (Stebich et al., 2009), we demonstrate the abrupt strengthening of the EASM, indicating there was an anti-phase between the two Asian monsoons during the YD period. We also describe both the spatial variation of precipitation in the EASM domain of the Chinese mainland and a typical representative region of the EASM strength variation. These results may provide the basis for a deeper understanding of the seemingly contradictory results described previously, and the global climate teleconnection.

2. Materials and methods

Hani peat mire (42°13′ N, 126°31′ E) is located in Liuhe county in the Jilin Province of northeast China (Fig. 1), and it is close to the so-called Northern Peatlands region. The annual average temperature is about 5.5 °C and the annual mean rainfall is about 750 mm in this area. Under the effect of the EASM, the regional vegetation is a temperate deciduous broadleaf-conifer mixed forest. The major plant population in the Hani peatland is the sedge family of C_3 plants, including *Carex*, *Eriophorum vaginatum*, and *Kobresia*. The peat deposit of some thick layers on the Chinese mainland always develops in relatively stable sedimentary environments (such as Ruoergai peat at the eastern edge of the Tibetan Plateau) , or in a crater lake (Jinchuan peat in the Jilin province), or a dammed lake (Hani peat in the Jilin province); thus, the floristic composition is relatively stable in term of the peat profile. The importance of the relative stability of the floristic composition was highlighted in particular during the study of Jinchuan peat, which revealed that more than 80% of the plant residue on the profile was composed of vascular sedges of C_3 plants, while the *Sphagnum* residue took up an extremely small proportion (Hong et al., 2000). Located in southeast, Hani peatland is about 15 km from the Jinchuan peatland, which belongs to the middle–low mountain bioclimatic zone, and the peat profile is also mainly composed of the vascular sedge family plants. Since the frost period persists for around 250 days and the freezing period is over half a year, the vegetation residue in peat decomposes slowly, resulting in the formation of a thick and continuous herbaceous peat deposition in a barrier lake formed by volcanic activity.

We drilled an 8.78 m-long peat core using a Russian Peat Corer. The core sample was cut contiguously into 1 cm subsamples corresponding to a mean time resolution of around 20 yr. We used an improved sodium chlorite oxidation method to extract alpha-cellulose from the peat vegetation residues (Green, 1963; Hong et al., 2000). About 20 mg of the cellulose sample can be extracted from every 1.5 g of the dry peat sample. We conducted measurements for ^{14}C, $\delta^{13}C$ and $\delta^{18}O$ in these cellulose samples. Around 2 mg of the cellulose samples was loaded into a borosilicate tube together with preheated copper (II) oxide. After drying under vacuum conditions, the tube was sealed with an oxy-gas torch and heated in a muffle

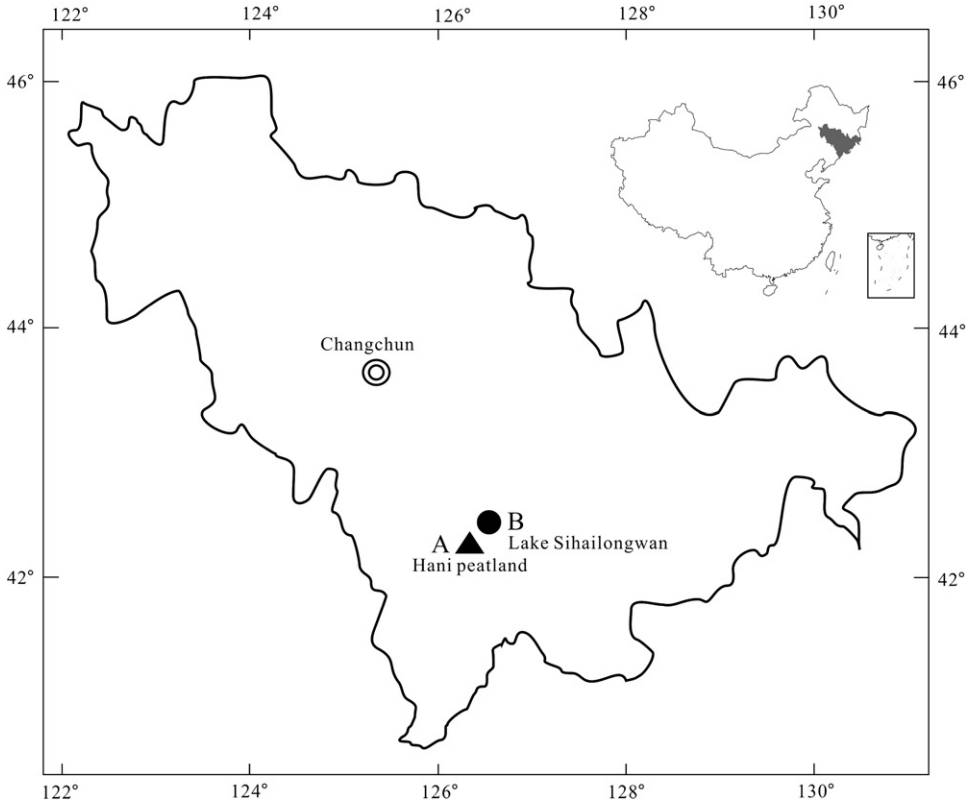

Fig. 1. Sketch map showing the location of research site. (A) and (B) indicate the location of Hani peat mire and Lake Sihailongwan in the Jilin Province, respectively. The upper right map shows the location of the Jilin Province in the mainland China.

furnace at 550 °C (Sofer, 1980; Hong et al., 2001). The resulting CO_2 gas was measured for stable isotopes using a MAT-252 mass spectrometer. The stable carbon isotopic composition of cellulose is expressed as $\delta^{13}C$ using the VPDB standard (Coplen, 1996) and the overall precision was found to be better than $\pm 0.1‰$ (1σ).

To build the ^{14}C age timescale, we first described the properties of the peat column samples collected on the field sampling spot and subdivided the column samples into several small fractions according to the colour and texture changes of the fresh peat samples. The colour and texture of each small fraction were the same; thus, correspondingly, the sedimentary environment and accumulative speed of each small fraction have been considered to be the same. Then we set up a ^{14}C age control point at the junction of two small column samples and added one ^{14}C age control point in some thicker small fractions of the column sample. Finally, a total of 13 ^{14}C age control points were set up (Fig. 2 of Hong et al., 2009). The peat cellulose samples of the control point were prepared for graphite targets, and their ^{14}C intensity was determined in the AMS Laboratory of the National Institute for Environmental Studies in Tsukuba, Japan, to obtain ^{14}C age; chronological age was obtained after correction using the CALIB-4.3 programme (Stuiver et al., 1998). We then obtained the chronological age sequence of the ^{14}C of Hani peat profile via the linear interpolation method (Hong et al., 2009). A total of 13 ^{14}C age data (Table 1) and a $\delta^{18}O$ time series of this 8.78 m-long peat core sample, and a $\delta^{13}C$ time series corresponding to the upper 7 m portion of the core sample (approximately corresponding to dates from 11200 to 0 cal.yr BP), have been previously published to document the earth surface temperature and the EASM in the Holocene, respectively (Hong et al., 2005, 2009).

Previous work has shown that vascular plants exhibit a sensitive physiological response to variations in water availability and the relative humidity of the environment by regulating the opening or closing of leaf stomata. This leads to changes in the stable carbon isotopic composition of atmospheric CO_2 utilized in photosynthesis (Francey and Farquhar, 1982; Schleser, 1995). Research has also revealed that the amount of rainfall is negatively correlated to the plant $\delta^{13}C$ value: the larger the amount of rainfall, the smaller the $\delta^{13}C$ value (Lee et al., 2005; Wang et al., 2008). As a result, information on monsoonal climatic changes at a given time is preserved in the $\delta^{13}C$ values of peat plant cellulose. Finally, plant cellulose is highly resistant to decomposition. Both cellulose and its isotopes are highly stable over periods of approximately 10^5 yr (Briggs et al., 2000). Therefore, the peat plant cellulose isotopes have significant potential as a bioindicator of paleoclimatic changes. Recent advances in extraction and purification of cellulose from batch-bulk peat samples have allowed application of the $\delta^{13}C$ value of peat plant cellulose to reconstruct the history of the Asian summer monsoons. The lower the amount of $\delta^{13}C$ in the peat cellulose, the higher the precipitation or intensity of the monsoon, and vice versa (Hong et al., 2003, 2005).

It can be expected that variations in precipitation would result in changes to vegetation and surface runoff. Fortunately, a high-resolution pollen record taken from the sediment of Lake Sihailongwan has been recently published (Stebich et al., 2009). Lake Sihailongwan (42°17′ N, 126°36′ E) is located about 15 km northeast of the Hani peat mire, and both the Hani peatland and Lake Sihailongwan are in the same bioclimatic zone. This provides a unique opportunity to compare the paleoclimate inferred from peat cellulose $\delta^{13}C$ and from pollen indicators.

Table 1
Radiocarbon dates of the Hani peat profile.

Lab no.	Depth (cm)	$\delta^{13}C$ (‰)	AMS ^{14}C age (^{14}C yr BP)	Selected cal. age range (1σ) (cal.yr BP)	Cal. age used in this study (cal.yr BP)
HA2	80	−26.10	807 ± 40	738–674	722
HA3	135	−26.78	1380 ± 88	1348–1193	1292
HA4	200	−25.81	2455 ± 46	2710–2358	2673
HA5	350	−26.22	4674 ± 53	5567–5318	5383
HA6	495	−26.97	7354 ± 63	8191–8041	8171
HA7	570	−27.98	7658 ± 64	8535–8389	8412
HA8	600	−27.02	8352 ± 76	9473–9163	9337
HA9	625	−26.84	9604 ± 80	11163–10745	10745
HA10	740	−27.13	10102 ± 80	11940–11344	11643
HA11	745	−26.94	10399 ± 89	12639–11966	12336
HA12	780	−26.53	10446 ± 91	12797–12127	12501
HA13	820	−26.27	11122 ± 90	13171–12999	13138
HA14	900	−27.43	11930 ± 172	14108–13658	13937

3. Results and discussion

3.1. Long-term change tendency of EASM

We present new data in Fig. 2A for the Hani peat cellulose $\delta^{13}C$ time series, during the period from about 11820 to 14200 cal.yr BP. This new data, combined with previous published data (Hong et al., 2005), provides a continuous proxy record for the history of the EASM strength variation over a span of approximately 14200 yr. The record clearly shows a long-term fluctuation. Starting from about 14000 cal. yr BP, the Hani $\delta^{13}C$ value decreased gradually, indicating that the EASM strength increased gradually, until it reached its maximum at about 10 000 cal.yr BP. Subsequently, the Hani $\delta^{13}C$ value increased gradually, indicating that the EASM strength weakened gradually. This long-term fluctuation of the monsoon strength coincides well with the orbital scale change of solar precession. Since the temperature gradient between ocean and land is the most basic condition underlying monsoon formation, we suggest that the temperature gradient variation resulting from the change in solar precession would fundamentally cause the EASM variation on an orbital scale.

3.2. Changes in EASM during the late-glacial period

It is noteworthy that the $\delta^{13}C$ time series of the Hani peat cellulose also showed a series of abrupt variations on centennial to millennial time scales. These variations are superimposed over the long-term changes seen in the EASM. In previous work, we discussed the abrupt variations of the EASM occurring since about 11820 cal.yr BP (Hong et al., 2005). In the present work, we focus on abrupt EASM variations in the late-glacial, especially during the YD cold period. In particular, we select the Hani peat cellulose $\delta^{13}C$ record during the period from 14200 to 10600 cal.yr BP as the research target (Fig. 2A). This time period coincides with the independent pollen record from Lake Sihailongwan sediments (Stebich et al., 2009), allowing comparison between the two data sets.

Fig. 2B shows the deviation from the mean of the Hani peat cellulose $\delta^{13}C$ series, during the period from 14200 to 10600 cal. yr BP. The zero line indicates −26.06‰; this is the mean of the peat cellulose $\delta^{13}C$ value over the entire profile of 14200 yr, and is almost equal to the average value of −26.17‰ for the section profile during the period from 14200 to 10600 cal.yr BP. However, we consider that the former mean value (over the entire period) is more reasonable. More negative peat cellulose $\Delta\delta^{13}C$ values are associated with a higher intensity of the EASM, and vice versa. Thus, the variations seen in the $\Delta\delta^{13}C$ value indicate that the EASM strength variation in the late-glacial can be divided into the four stages described in the next section.

3.2.1. Weakening EASM activity during the Bølling–Allerød warming period

In Fig. 2B, the peat $\Delta\delta^{13}C$ values in the period from around 14200 to 13700 cal.yr BP are obviously higher than the mean value; this indicates less rainfall or a weak intensity EASM. This may be the

period of weakest monsoon activity over the entire 14200 yr. Also, according to the Hani peat cellulose $\delta^{18}O$ record (Fig. 2C), the surface temperature of the region was warmer in this period than it was in the late-Bølling and early Allerød periods. Thus, based on the peat cellulose isotope records, the general climatic condition during this period would be relatively warmer and dryer than the mean conditions, which differs from the warmer and wetter condition in the IOSM area during the same period (Sinha et al., 2005).

The period examined here overlaps with the second stage of the pollen record from Lake Sihailongwan sediments (Fig. 2E). There is evidence during this stage of the appearance and minimal increase in some more thermophilous taxa, such as *Syringa, Juniperus, Salix, Rosaceae, Thalictrum* and *Filipendula*, and in some drought-tolerance taxa, such as *Ulmus pumila* and *Quercus mongolica.* However, *Betula Artemisia* and *Poaceae* continue to dominate the pollen spectra, indicating that the broadleaved forests of (cool) temperate zones appeared in this area. Despite this, the more cold-tolerant and hygrophilous taxa, such as *Picea*, *Larix*, and *Abies,* almost completely disappeared subsequent to the initial late-glacial vegetation change. The forest coverage was also smaller (Stebich et al., 2009). It is noteworthy that at around 14200 cal. yr BP, the pollen influx increased rapidly, and varved sediment distinctly thickened (Fig. 2D), indicating increases of biogenic and minerogenic components. Researchers have speculated that variations in the sedimentary process may correspond to high precipitation levels and the substantial thawing of local permafrost (Stebich et al., 2009). However, as indicated by the Hani peat record, the $\Delta\delta^{13}C$ value at around 14200 cal. yr BP has an obvious increased peak, which indicates low precipitation levels. Thus, there appears to be little possibility of a rainfall increase in the period. The variation is more likely attributed to the high surface temperature in the Bølling period as indicated by the Hani peat $\delta^{18}O$ record (Fig. 2C) (Hong et al., 2009). With a relatively open landscape, the Bølling–Allerød warm period, lasting as long as 400 yr, likely triggered a vast melting of the local permafrost, leading to an increase of groundwater flow, the instability of the soil horizon, an increase of the erosion effect, and finally, the enhancement of the varve thickness.

3.2.2. Fluctuation of EASM in the late Allerød

As Fig. 2B shows, compared with the previous stage the peat $\Delta\delta^{13}C$ value obviously decreases over the 1000 yr period from around 13700 to 12700 cal. yr BP. This indicates that the EASM has strengthened and rainfall has increased. However, in general the peat $\Delta\delta^{13}C$ values show repeated slight up and down fluctuations near the mean value. There would be a moderate alternation between wet and dry, and the characteristic EASM activity during this period would be mild oscillation around the mean value. Thus, the climatic condition in this area is close to the perennial average state; a sustained sudden dramatic climate change is not obvious.

As supported by the Lake Sihailongwan pollen record, this long-term mild oscillation of EASM intensity would not cause any abrupt and significant changes to the vegetation and environment. Fig. 2E indicates that over this long period, the percentage of woody and herbaceous vegetations seen in the Lake Sihailongwan pollen record is relatively stable (Stebich et al., 2009). The research also shows that, compared with the last pollen diagram stage, the most striking feature of the considered stage is the much higher percentage of the broadleaf tree taxa *Ulmus* and *Fraxinus*. Other thermophilous taxa, such as *Corylus*, *Quercus*, *Viburnum*, and *Ostryopsis*, occurred regularly. Heliophilous taxa, such as *Artemisia* and *Thalictrum*, remain abundant, indicating the existence of openings within the late-glacial forested landscape. However, this differs from the vegetation changes that do not correspond to changes in the varve thickness of Lake Sihailongwan and the geochemical index during this period. Therefore, the research suggests that the change in the dominant tree taxa in this period is unlikely triggered by a climatic shift, but instead is the result of inherent rates of population increase (Stebich et al., 2009), which coincide with the long-term mild oscillation of the EASM.

3.2.3. Abrupt strengthening of EASM during the YD cold period

Earlier results indicated that during the time of the YD cold period in Europe and North America, the temperature in the West Pacific Ocean region also displayed an obvious decrease (Stott et al., 2002). This climatic deterioration also appeared in the Hani-Lake Sihailongwan region. Examining the variation in vegetation and environment at Lake Sihailongwan (Fig. 2E), it can be seen that in the period from around 12 700 to 11700 cal. yr BP, the percentage of thermophilous taxa, such as *Ulmus* and *Fraxinus*, decreased significantly and abruptly, combined with the maximal percentage of cold-tolerant *Betula* and *Picea*. Moreover, the accumulation rate of pollen and the content of total organic carbon (TOC) were relatively low. Thus, these results clearly reveal a rapid and substantial cooling during the YD (Stebich et al., 2009), which generally coincides with the temperature decrease inferred from the Hani peat cellulose $\delta^{18}O$ record (Hong et al., 2009).

However, the monsoonal precipitation in this region during the YD needs further clarification. Fig. 2E shows an important feature of the pollen composition in this period: the percentages of *Larix, Picea*, and *Abies* reach their maximum for the first time during the entire study period. This generally indicates an increase of wetness. In addition, the pollen percentage of *Cyperaceae*, which generally increases in the wet environment around the lake, is also at a maximum. This might indicate a higher lake level. Particularly, the thickness of the sediment varve of Lake Sihailongwan drastically oscillates, with series maximum peaks occurring that are up to two centimeters. These phenomena have been attributed to enhanced surface runoff and comparatively unsettled climatic conditions during this interval (Stebich et al., 2009).

Although there are many factors that can cause an increase of surface runoff, for example, the re-appearance of permafrost, reduced vegetation cover, and resultant unstable soils, these factors mainly reflect the shift of background landform features. They do not indicate the dynamic reason behind the abrupt changes in the sediment. We consider that an abrupt increase in the rainfall amount would be the first basic dynamic reason for the enhanced varve thickness. The peat cellulose $\delta^{13}C$ record provides evidence for this. Fig. 2B shows that since around 12700 cal. yr BP, there is a transition from a stage lasting 1000 yr where the peat $\Delta\delta^{13}C$ shows repeated and slight fluctuations near the mean, to another 1000 yr stage where the levels are predominantly on the negative side of the mean. This is probably not related to the variations of atmospheric CO_2 during the YD. The determination of CO_2 trapped in Antarctic ice cores has shown that while the concentration of atmospheric CO_2 increased from around 200 to 280 ppmv in the period from 15000 to 10000 cal. yr BP, the $\delta^{13}C$ value of atmospheric CO_2 increased correspondingly from around −6.9 to −6.4 ‰ (Marino and McElroy, 1991). The influence of this more positive $\delta^{13}C$ shift of atmospheric CO_2 on the $\delta^{13}C$ value of C_3 plants is negligible, particularly in our case since the $\delta^{13}C$ of peat cellulose showed the more negative shift during the YD period. Some previous studies have also indicated that the response of carbon isotope composition of C_3 plants to Pleistocene long-term pCO_2 variations (360–280 ppmv) is rather minimal (Tu et al., 2004). Therefore, the more negative peat $\delta^{13}C$ values should be attributed to the EASM abruptly strengthened and the precipitation concurrently increased in YD. Moreover, the peak values of precipitation indicated by Hani peat $\Delta\delta^{13}C$ correspond well to the enhanced varve thickness of Lake Sihailongwan in general. This suggests that the increased rainfall may enhance the surface runoff and exacerbate soil erosion, which results in an increased supply of allochthonous minerogenic material leading to the enhancement of the varve thickness in Lake Sihailongwan. However, rainfall seems not to be the only reason for enhanced varve thickness, because there is no one-to-one correspondence between the variations in precipitation and the varve thicknesss. This may imply that the buffer effect of permafrost in the soil should also be considered (Camill and Clark, 1998; Stebich et al., 2009). In fact, starting

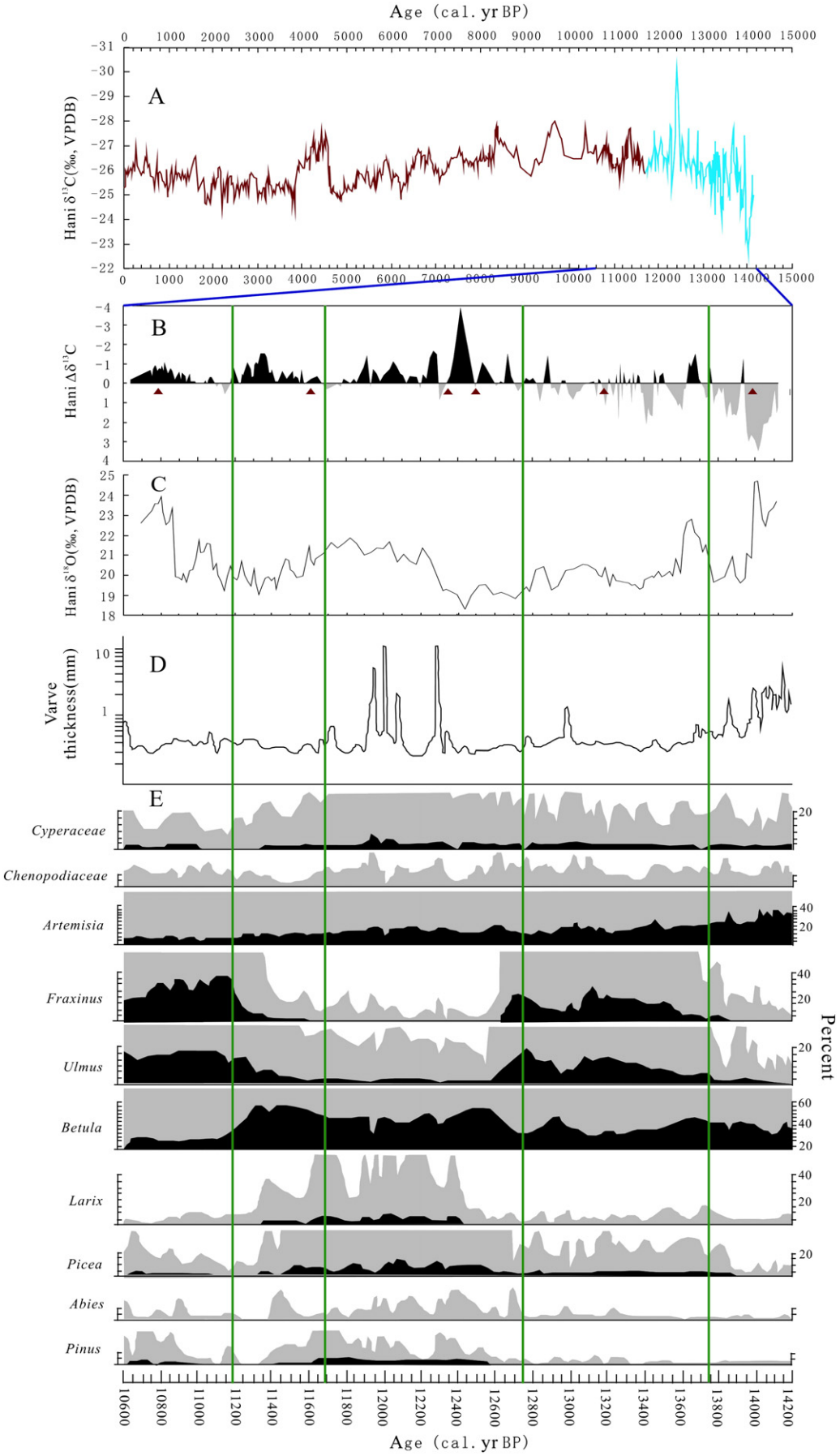
Age (cal. yr BP)
A
Hani δ13C(‰, VPDB)
B
Hani Δδ13C
C
Hani δ18O(‰, VPDB)
D
Varve thickness(mm)
E
Cyperaceae
Chenopodiaceae
Artemisia
Fraxinus
Ulmus
Betula
Larix
Picea
Abies
Pinus
Percent
Age (cal. yr BP)

from about 12700 cal.yr BP, both the Hani peat $\delta^{18}O$ record and the Greenland GISP2 records indicate a rapid temperature drop, with the temperature reaching a minimum at about 12 500 cal.yr BP (Hong et al., 2009). This may have led to the formation of permafrost in the soil at the Hani–Lake Sihailongwan region. Thus, in spite of the occurrence of large rainfall amounts inferred from the clearly seen peak in peat $\Delta\delta^{13}C$ values around 12500 cal.yr BP, the existence of permafrost may have buffered the soil erosion so that a thick varve did not form in the Lake Sihailongwan sediment. At a later time, the Hani peat cellulose $\delta^{18}O$ record indicates that in the period from around 12400 to 11900 cal. yr BP, similar to what happened in Europe, the temperature of the region rose gradually, and the climatic condition underwent amelioration to a certain degree (Fig. 2C); this has been construed as a warm event (Genty et al., 2006; Hong et al., 2009). As this may lead to some melting of the permafrost at the Hani–Lake Sihailongwan region, the soil layer could have become unstable. Combined with enhanced rainfall, the reduced buffer effect due to decreased permafrost could lead to rainfall erosion. More minerogenic and organic materials would have been transported into the lake, leading to enhanced varve thickness.

In summary, during the YD cold period the Hani peat cellulose $\delta^{13}C$ value displayed a continuous and obvious decrease, indicating an increase in the rainfall amount and an increase in intensity of the EASM. This cold-wet climatic feature is in general consistent with the climatic condition indicated by the pollen assembly of cold-tolerance *Betula* and hygrophilous *Abies*, *Larix*, and *Picea*, as well as by an obvious increase in varve thickness at Lake Sihailongwan.

3.2.4. Abrupt strengthening of EASM in the IRD-8 cold event

As indicated in Fig. 2B, the Hani peat $\Delta\delta^{13}C$ record showed an increase over a short period in the late YD, indicating that the intensity of the EASM gradually decreased, returning to its mean value. From around 11700 cal.yr BP, the EASM gradually strengthened again until around 11200 cal.yr BP. Over this period, the Hani peat $\delta^{18}O$ record shows an obvious cooling of the temperature (Fig. 2C), which corresponds to the No. 8 ice-rafted debris event of the North Atlantic (IRD-8 event). Some research results have revealed that, corresponding to the IRD events in the Holocene, including an IRD-8 event, the intensity of the EASM strengthened and IOSM weakened (Hong et al., 2005; Schettler et al., 2006). It can be seen from Fig. 2 that the pollen composition of Lake Sihailongwan in this period is nearly consistent with that from the YD. But the largest difference is the absence of an obvious increase in varve thickness, which may be related to the low surface temperature and to permafrost which stabilizes the soil.

3.3. Spatial variation and representative region of EASM intensity

The Asian summer monsoon includes two monsoonal systems, IOSM and EASM. Although they form independently of each other, these interactive climatic systems both play an important role in water vapor transport and summer precipitation on the East Asian continent (Tao and Chen, 1987). Therefore, it is important to distinguish the regions that are influenced by these two monsoons, and in particular to identify any region that sensitively reflects the EASM intensity through its rainfall. Unfortunately, investigations into the monsoonal division of the East Asian continent have been insufficient so far (Hong et al., 2006), although a framework for the Chinese Mainland was presented in 1962 (Gao et al., 1962). In general, meteorologists consider the area east of the 105° E longitude line to be the EASM domain, and the area west of that line, particularly the Tibetan plateau region (Sun, 1996), to be the IOSM domain (Gao et al., 1962; Wang et al., 2003).

However, it is worth emphasizing that there is a significant spatial and temporal variability in the rainfall amount and in the intensity of EASM over the Chinese mainland. In general, in April or May of every spring, a monsoonal rainbelt situates over the South China Sea region. In late May or early June, a rainbelt moves to the region south of the Yangtze River. Then, a rainbelt will suddenly jump northward to the region of the Yangtze River-Huaihe River basin in the Chinese mainland, Japan and South Korea. This marks the beginning of the Meiyu season in China's Yangtze River–Huaihe River basin, and of Japan's Baiu and South Korean's Changma season. In early or middle July, a rainbelt of the monsoon will again jump northward to a region in north China, northeast China, and North Korea, indicating the end of Meiyu season in the Yangtze River–Huaihe River region and the beginning of the rainy season in the northern regions of China. After the middle of August, a monsoonal rainbelt generally moves quickly back to southern China. This phenomenon shows the so-called three settlements and two skip motions of a monsoonal rainbelt over the Chinese mainland (Huang et al., 2008).

Therefore, the distribution of the rainfall amount over the Chinese mainland depends on the moving speed of a monsoonal rainbelt, and on the length of time it remains over a given position. This often results in anomalous rainfall patterns on interannual time scales, with either floods in the north and drought in the south, or drought in the north and floods in the south of the Chinese mainland. For example, during the period from 1951 to 1965, precipitation in north China was much higher than the perennial mean value. From 1965 to 1976, it began to show oscillations. Starting around 1977, the rainfall obviously decreased, and a continuous drought condition has occurred in north China (Huang et al., 2008).

Results from numerical analysis and modeling have revealed that the anomalous precipitation distribution over the Chinese mainland on the interannual scale is related closely to both the intensity and position of the Western Pacific subtropical high (STH) and the thermal condition of the Equatorial Pacific. The interannual variation of the STH reflects the variation in the EASM intensity. When the SST variation in the Equatorial Pacific takes on an El Niño-like pattern, the STH tends to strengthen. This is accompanied by a strengthened ITCZ, and generally results in stronger convection, especially over the tropical Western Pacific. In this case, the STH over the Western Pacific moves to the north, resulting in a migration of a precipitation belt to the north of the Chinese continent. This results in an increase in rainfall in both the north and northeast regions of China, and concurrently, less rainfall in the middle and lower regions of the Yangtze River. Conversely, when the SST variation in the Equatorial Pacific takes on a La Niña-like pattern, the STH intensity tends to weaken, and its location over the Western Pacific moves to the south. This generally results in a migration of a precipitation belt to the southern regions of the Chinese continent, with an increase in precipitation in the south, but less rainfall in the north and northeast (Sun and Ying, 1999; Ying and Sun, 2000; Wu et al., 2003). Since only a strong EASM that originates from the South China Sea can expand to northern China and can remain there for a long time, meteorologists commonly regard precipitation conditions in north and northeast China as typically representative of the strength variation of the EASM (Gao et al., 1962; Wang and Zhu, 2006). This implies that more or less

Fig. 2. Comparison between the climatic conditions inferred respectively from the Hani peat cellulose $\delta^{13}C$, $\delta^{18}O$ and Lake Sihailongwan sediment record. (A) A continuous Hani peat cellulose $\delta^{13}C$ record spanning around 14200 years, in which red curve denotes its sectional record that has been published in previous works (Hong et al., 2005), and blue curve denotes the new data presented in this article. (B) The deviation from the mean of the Hani peat cellulose $\delta^{13}C$ series during the period from 14200 to 10600 cal. yr BP. The red triangles show calibrated ^{14}C age control points that have been published in previous works (Hong et al., 2009). (C) The Hani peat cellulose $\delta^{18}O$ record (Hong et al., 2009). (D) The varve thickness of Lake Sihailongwan (Stebich et al., 2009). (E) Simplified pollen influx diagram covering the period of investigation (Stebich et al., 2009), in which exaggeration ($\times 10$) is indicated by grey shadow.

precipitation in north and northeast China generally indicates a stronger or weaker EASM, respectively, although other regions of the Chinese continent may not necessarily show the same precipitation condition at the same time.

The variation of EASM strength in the YD period may provide further paleoclimatic evidence for monsoon activity. Fig. 3 shows research results for the intensity variation of the two Asian monsoons in the YD period. In the western Chinese mainland affected by the IOSM, the monsoonal precipitation inferred by multiple proxy indicators had decreased, and the IOSM became weak (Gasse et al., 1991; Jarvis, 1993; Li et al., 1994), which coincided with the climatic condition of the Indian subcontinent and Arabian Sea regions (Sirocko et al., 1996; Schulz et al., 1998; Sinha et al., 2005). However, precipitation in the EASM domain showed a different distribution. The region north of Huaihe River received a lot of precipitation in general (Wang et al., 1994; Stebich et al., 2009), and the region south of Huaihe River received less precipitation (Wang et al., 1999, 2001; Huang et al., 2009; Zhong et al., 2010). This may reveal that during the YD, the position of a monsoonal rainbelt more often moved to the north, resulting in the anomalous rainfall mode with wet in the north and dry in the south. As mentioned before, this would reflect the strengthening of the EASM. In particular, strengthening the EASM not only transports plenty of moisture to north and northeast China, but also transports moisture to northwest China (Kelts et al., 1989; An et al., 1993; Zhou et al., 1996), even to the regions of Lake Bosten and Lake Manas in the Xinjiang Province along the northeast edge of the Qinghai–Tibet Plateau (Rhodes et al., 1996; Zhong, 1998). This resulted in an increase of precipitation and higher lake levels of the regions. In contrast, it was during this period that the Hulu cave stalagmite situated in the lower reaches of Yangtze River recorded a decrease of monsoon rainfall (Wang et al., 2001). Also, the salinity increased and the amount of biogenic silicon decreased in the South China Sea, as recorded by the No. 17940 sediment core. This has been attributed to the decrease in precipitation in the south china region, resulting in less fresh water through the Pearl River inputting to the South China Sea (Wang et al., 1999; Huang et al., 2009). Therefore, the seemingly contradictory results regarding the different precipitation conditions in fact should be considered to demonstrate the strengthening of the EASM during the YD.

The climatologically dynamic reason for the anomalous precipitation mode of wet in the north and dry in the south during YD may also be a direct result of the occurrence of an El Niño-like pattern in the Equatorial Pacific, though the influence of meltwater on the thermal condition of the Equatorial Pacific remains unclear. Research on the cold tongue of the Equatorial Pacific has shown that, during the YD, the SST gradient decreased and was in an El Niño-like pattern (Koutavas et al., 2002). Possibly this resulted in anomalous strengthening of both the STH over the Western Pacific and the EASM. Consequently, the anomalous precipitation distribution appeared (wet in the north and dry in the south of the Chinese mainland). Since the IOSM weakened during the YD period, the intensity of the two Asian monsoons showed anti-phase variations resulted from the thermal condition variation of the Equatorial Pacific Ocean.

4. Conclusions

(1) In general, records from both the Hani peat cellulose isotope and the Sihailongwan lake pollen indicate the same phenomenon, that the climate of the YD cold period in northeastern China is wet, having increased precipitation.

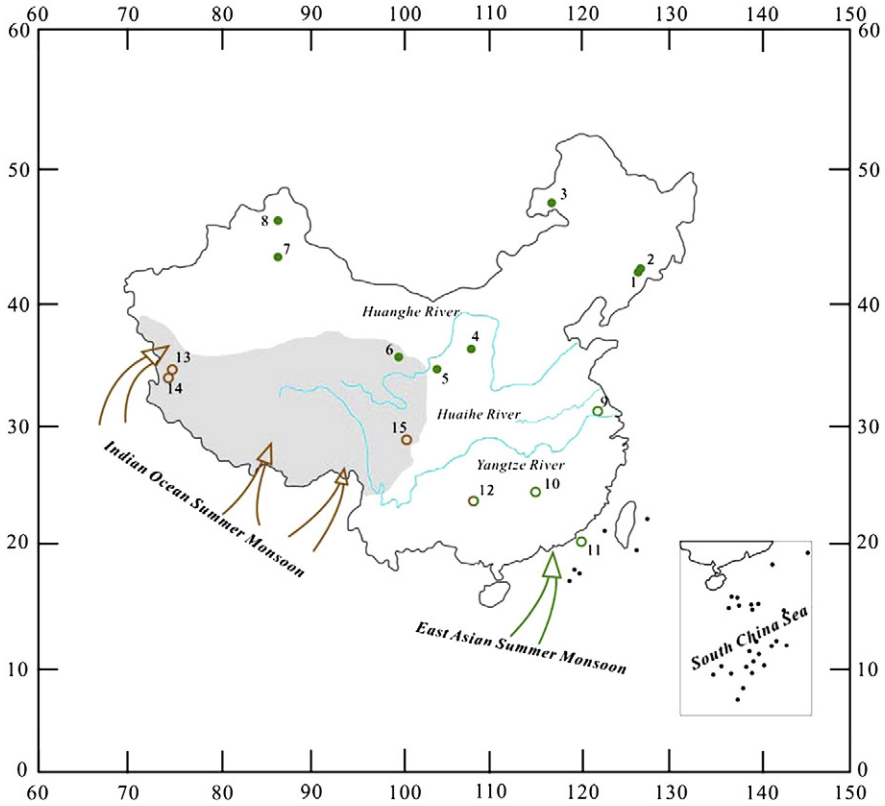

Fig. 3. Sketch map showing the location of research site for monsoonal precipitation on the Chinese Mainland during the Younger Dryas period. Yellow circle denotes the site with dry climatic conditions influenced by the Indian Ocean Summer Monsoon. Green solid circle and green circle denote the sites with wet and dry climatic conditions influenced by the East Asian Summer Monsoon, respectively. Yellow/green circle denotes the site with dry climatic conditions influenced by the Asian monsoon. 1—Hani peat mire; 2—Lake Sihailongwan (Stebich et al., 2009); 3—Lake Zalairoer (Wang et al., 1994); 4—Midiwan paleosol sequences (Zhou et al., 1996); 5—Baxie loess (An et al., 1993); 6—Lake Qinghai (Kelts et al., 1989); 7—Lake Bosten (Zhong, 1998); 8—Lake Manas (Rhodes et al., 1996); 9—Hulu Cave (Wang et al., 2001); 10—Dahu Swamp (Zhong et al., 2010); 11—Core 17940, South China Sea (Wang et al., 1999); 12—Dongge Cave (Yuan et al., 2004); 13—Lake Sumxi Co (Gasse et al., 1991); 14—Lake Banggong Co (Li et al., 1994); 15—Lake Shayema (Jarvis, 1993).

(2) During the YD period, the precipitation increased in the wide regions north of the Huaihe River, including northwestern China. In contrast, the precipitation generally decreased in the middle and lower regions of the Yangtze River and in the region south of the Yangtze River. This kind of anomalous rainfall distribution is similar to the anomalous distribution of wet in the north and dry in the south over the Chinese mainland on an interannual scale. It is possible that their dynamic forcing would be attributed to the occurrence of SST variations from the El Niño-like pattern in the Equatorial Pacific Ocean, although the relationship between meltwater and the thermal condition of the Equatorial Pacific still need to be studied further. Correspondingly, the STH strengthened and its position over the western Pacific Ocean moved to the north. In this case, the EASM was enhanced, and a monsoonal rainbelt migrated to the north region of the Chinese mainland, resulting in the anomalous precipitation distribution described earlier. Thus, this anomalous rainfall distribution indicates the strengthening of EASM, and an anti-phase variation corresponding to the weakening of IOSM in this period.

(3) These phenomena (strengthening of the EASM and weakening of the IOSM) during the YD cold event agree with the previously revealed results of the two monsoon intensity variations during the IRD cold events. They all demonstrate that, corresponding to the abrupt temperature drop in the Northern Hemisphere on the centennial to millennial time scale, anti-phase variations of the two Asian summer monsoons occurred. These results provide new evidence for the conceptual model of teleconnections between the Asian monsoons, the anomalous surface temperature of the Northern Hemisphere, and the SST variation of the Equatorial Pacific.

(4) The Hani peat cellulose $\delta^{13}C$ data published here, together with previous published data, constitute a proxy record of EASM strength variation lasting for around 14,200 yr. The indicated long-term fluctuation of monsoon strength coincides well with the change of solar precession on an orbital scale.

Acknowledgements

We sincerely thank Thierry Corrège and three anonymous reviewers for their insightful comments and constructive suggestions. This work was supported by the National Natural Science Foundation of China (grant No. 40973089, 40573004 and 40231007).

References

Alley, R.B., 2000. The Younger Dryas cold interval as viewed from central Greenland. Quat. Sci. Rev. 19, 213–226.

An, Z.S., Porter, S.C., Zhou, W.J., Lu, Y.C., Donahue, D.J., Head, M.J., Wu, X.H., Ren, J.Z., Zheng, H.B., 1993. Episode of strengthened summer monsoon climate of Younger Dryas age on the loess plateau of central China. Quat. Res. 39, 45–54.

Bond, G., Showers, W., Cheseby, M., Lotti, R., Almasi, P., deMenocal, P., Priore, P., Cullen, H., Hajdas, I., Bonani, G., 1997. A pervasive millennial-scale cycle in North Atlantic Holocene and glacial climates. Science 278, 1257–1266.

Bond, G., Kromer, B., Beer, J., Muscheler, R., Evans, M.N., Showers, W., Hoffmann, S., Lotti-Bond, R., Hajdas, I., Bonani, G., 2001. Persistent solar influence on North Atlantic climate during the Holocene. Science 294, 2130–2136.

Briggs, D.E.G., Evershed, R.P., Lockheart, M.J., 2000. The biomolecular paleontology of continental fossils. Paleobiology 26, 169–193.

Broecker, W.S., 2003. Does the trigger for abrupt climate change reside in the ocean or in the atmosphere? Science 300, 1519–1522.

Broecker, W.S., Peteet, D.M., Rind, D., 1985. Does the ocean–atmosphere system have more than one stable mode of operation? Nature 315, 21–25.

Camill, P., Clark, J.S., 1998. Climate change disequilibrium of boreal permafrost peatlands caused by local processes. Am. Nat. 151, 207–222.

Clement, A.C., Peterson, L.C., 2008. Mechanisms of abrupt climate change of the last glacial period. Rev. Geophys. 46, RG4002. doi:10.1029/2006RG000204.

Coplen, T.B., 1996. New guidelines for reporting stable hydrogen, carbon, and oxygen isotope-ratio data. Geochmica et Cosmochimica Acta 60, 3359–3360.

Francey, R.J., Farquhar, G.D., 1982. An explanation of $^{13}C/^{12}C$ variations in tree rings. Nature 297, 28–31.

Gao, Y.X., Xu, S.Y., Guo, Q.Y., 1962. Monsoon region and reginal climate in China. In: Gao, Y.X., Xu, S.Y. (Eds.), Some Problems of East Asian monsoon (in Chinese). Science Press, Beijing, pp. 49–63.

Gasse, F., Arnold, M., Fontes, J.C., Fort, M., Gibert, E., Huc, A., Li, B.Y., Li, Y.F., Liu, Q., Mélières, F., Campo, E.V., Wang, F.B., Zhang, Q.S., 1991. A 13,000-year climate record from western Tibet. Nature 353, 742–745.

Genty, D., Blamart, D., Ghaleb, B., Plagnes, V., Causse, Ch., Bakalowicz, M., Zouari, K., Chkir, N., Hellstrom, J., Wainer, K., Bourges, F., 2006. Timing and dynamics of the last deglaciation from European and North African $\delta^{13}C$ stalagmite profiles—comparison with Chinese and South Hemisphere stalagmites. Quat. Sci. Rev. 25, 2118–2142.

Green, J.W., 1963. Wood cellulose. In: Whistler, R.L. (Ed.), Methods in Carbohydrate Chemistry, 3. Academic Press, New York, pp. 9–22.

Hong, B., Lin, Q.H., Hong, Y.T., 2006. Interconnections between the Asian monsoon, ENSO, and high northern latitude climate during the Holocene. Chinese. Sci. Bull. 51, 2169–2177.

Hong, Y.T., Jiang, H.B., Liu, T.S., Zhou, L.P., Beer, J., Li, H.D., Leng, X.T., Hong, B., Qin, X.G., 2000. Response of climate to solar forcing recorded in a 6000-year$\delta^{18}O$ time series of Chinese peat cellulose. Holocene 10, 1–7.

Hong, Y.T., Wang, Z.G., Jiang, H.B., Lin, Q.H., Hong, B., Zhu, Y.X., Wang, Y., Xu, L.S., Leng, X.T., Li, H.D., 2001. A 6000-year record of changes in drought and precipitation in northeastern China based on a $\delta^{13}C$ time series from peat cellulose. Earth Planet. Sci. Lett. 185, 111–119.

Hong, Y.T., Hong, B., Lin, Q.H., Zhu, Y.X., Shibata, Y., Hirota, M., Uchida, M., Leng, X.T., Jiang, H.B., Xu, H., Wang, H., Yi, L., 2003. Correlation between Indian Ocean summer monsoon and North Atlantic climate during the Holocene. Earth Planet. Sci. Lett. 211, 371–380.

Hong, Y.T., Hong, B., Lin, Q.H., Shibata, Y., Hirota, M., Zhu, Y.X., Leng, X.T., Wang, Y., Wang, H., Yi, L., 2005. Inverse phase oscillations between the East Asian and Indian Ocean summer monsoons during the last 12000 years and paleo-El Niño. Earth Planet. Sci. Lett. 231, 337–346.

Hong, Y.T., Hong, B., Lin, Q.H., Shibata, Y., Zhu, Y.X., Leng, X.T., Wang, Y., 2009. Synchronous climate anomalies in the western North Pacific and North Atlantic regions during the last 14,000 years. Quat. Sci. Rev. 28, 840–849.

Huang, R.H., Gu, L., Chen, J.L., Huang, G., 2008. Recent progress in studies of the temporal–spatial variations of the East Asian monsoon system and their impacts on climate anomalies in China. Chinese J. Atmos. Sci. 32, 691–719 (in Chinese with English summary).

Huang, Y., Jiang, H., Sarnthein, M., Knudsen, K.L., Li, D.L., 2009. Diatom response to changes in palaeoenvironments of the northern South China Sea during the last 15000 years. Mar. Micropleo. 72, 99–109.

Jarvis, D.I., 1993. Pollen evidence of changing Holocene monsoon climate in Sichuan province. China. Quat. Res. 39, 325–337.

Kelts, K., Chen, K.Z., Lister, G., Yu, J.Q., Gao, Z.H., Nissen, F., Bonani, G., 1989. Geological fingerprints of climate history: a cooperative study of Qinghai Lake. China. Eclogae geol. Helv. 82, 167–182.

Knutti, R., Fluckiger, J., Stocker, T.F., Timmermann, A., 2004. Strong hemispheric coupling of glacial climate through freshwater discharge and ocean circulation. Nature 430, 851–856.

Koutavas, A., Lynch-Stieglitz, J., Marchitto Jr., T.M., Sachs, J.P., 2002. El Niño-like pattern in Ice Age tropical Pacific sea surface temperature. Science 297, 226–230.

Lee, X.Q., Feng, Z.D., Guo, L.L., Wang, L.X., Jin, L.Y., Huang, Y.S., Chopping, M., Huang, D., Jiang, W., Jiang, Q., Cheng, H.G., 2005. Carbon isotope of bulk organic matter: a proxy for precipitation in the arid and semiarid central East Asian. Global Biogeochem. Cycles 19, GB4010. doi:10.1029/2004GB002303.

Li, Y.F., Zhang, Q.S., Li, B.Y., 1994. Ostracod fauna and environmental changes during the past 17000 years in the western Tibet. Acta. Geog. Sin. 49, 46–54 (in Chinese with English summary).

Marino, B.D., McElroy, M.B., 1991. Isotopic composition of atmospheric CO_2 inferred from carbon in C_4 plant cellulose. Nature 349, 127–131.

Rhodes, T.E., Gasse, F., Lin, R.F., Fontes, J.C., Wei, K.Q., Bertrand, P., Gibert, E., Mélières, F., Tucholka, P., Wang, Z.X., Cheng, Z.Y., 1996. A late Pleistocene–Holocene lacustrine record from Lake Manas, Zunggar (northern Xinjiang, western China). Paleogeogr. Paleoclimatol. Paleoecol. 120, 105–121.

Roberts, N., Taieb, M., Barker, P., Damnati, B., Icole, M., Williamson, D., 1993. Timing of the Younger Dryas event in East Africa fromlake-level changes. Nature 366, 146–148.

Rooth, C.G.H., 1982. Hydrology and ocean circulation. Prog. Oceanogr. 11, 131–149.

Schettler, G., Liu, Q., Mingram, J., Stebich, M., Dulski, P., 2006. East-Asian monsoon variability between 15000 and 2000 cal. yr BP recorded in varved sediments of Lake Sihailongwan (northeastern China, Long Gang volcanic field). Holocene 16, 1043–1057.

Schleser, G.H., 1995. Parameters determining carbon isotope ratios in plants. In: Frenzel, B., Stauffer, B., Weiss, M.M. (Eds.), Paläoklimaforschung, 15. Strasbourg, France, pp. 71–96.

Schulz, H., von Rad, U., Erlenkeuser, H., 1998. Correlation between Arabian Sea and Greenland climate oscillations of the past 110,000 years. Nature 393, 54–57.

Sinha, A., Cannariato, K.G., Stott, L.D., Li, H.-C., You, C.-F., Cheng, H., Edwards, L., Singh, B., 2005. Variability of south-west Indian summer monsoon precipitation during the Bølling–Allerød. Geology 33, 813–816.

Sirocko, F., Garbe-Schönberg, D., McIntyre, A., Molfino, B., 1996. Teleconnections between the subtropical monsoons and high-latitude climates during the last deglaciation. Science 272, 526–529.

Sofer, Z., 1980. Preparation of carbon dioxide for stable carbon isotope analysis of petroleum fractions. Anal. Chem. 52, 1389–1391.

Stebich, M., Mingram, J., Han, J.T., Liu, J.Q., 2009. Late Pleistocene spread of (cool-) temperate forests in northeast China and climate changes synchronous with the North Atlantic region. Global Planet. Change 65, 56–70.

Stott, L., Poulsen, C., Lund, S., Thunell, R., 2002. Super ENSO and global climate oscillations at millennial time scales. Science 297, 222–226.
Stuiver, M., Reimer, P.J., Bard, E., Beck, J.W., Burr, G.S., Hughen, K.A., Kromer, B., McCormac, F.G., Plicht, J.V.D., Spurk, M., 1998. Radiocarbon calibration program rev 4.3. Radiocarbon 40, 1041–1083.
Sun, H., 1996. Formation and Evalution of Qinghai–Xizang Plateau. Shanghai Press, Shanghai, pp. 101–146.
Sun, S.Q., Ying, M., 1999. Subtropical high anomalies over the Western Pacific and its relations to the Asian monsoon and SST anomaly. Adv. Atmos. Sci. 16, 559–568.
Tao, S., Chen, L., 1987. A review of recent research on the East Asian summer monsoon in China. In: Chang, C.P., Krishnamurti, T.N. (Eds.), Monsoon Meteorology. Oxford University Press, Oxford, pp. 60–92.
Teller, J.T., Leverington, D.W., Mann, J.D., 2002. Freshwater outbursts to the oceans from glacial Lake Agassiz and their role in climate change during the last deglaciation. Quat. Sci. Rev. 21, 879–887.
Tu, T.T.N., Kurschner, W.A., Schouten, S., Van Bergen, P.F., 2004. Leaf carbon isotope composition of fossil and extant oaks grown under differing atmospheric CO_2 levels. Paleogeogr. Paleoclimatol. Paleoecol. 212, 199–213.
Wang, B., Clemens, S.C., Liu, P., 2003. Contrasting the Indian and East Asain monsoon: implications on geological timescles. Mar. Geol. 201, 5–21.
Wang, G., Feng, X., Han, J., Zhou, L., Tan, W., Su, F., 2008. Paleovagetation reconstruction using $\delta^{13}C$ of soil organic matter. Biogeosciences 5, 1325–1337.
Wang, L., Sarnthein, M., Erlenkeuser, H., Grimalt, J., Grootes, P., Heilig, S., Ivanova, E., Kienast, M., Pelejero, C., Pflaumann, U., 1999. East Asian monsoon climate during the Late Pleistocene: high-resolution sediment records from the South China Sea. Mar. Geol. 156, 245–284.
Wang, S.M., Ji, L., Yang, X.D., Xue, B., Ma, Y., Hu, S.Y., 1994. The record of Younger Dryas event from sediment in Zalairoer Lake, Inner Mongolia. Chin. Sci. Bull. 39, 348–351.
Wang, S.W., Zhu, J.H., 2006. Studies of the chronology of millennial time scale climate oscillations in the Holocene. Adv. Clim. Change Res. 1 (4), 1673–1719.
Wang, Y.J., Cheng, H., Edwards, R.L., An, Z.S., Wu, J.Y., Shen, C.-C., Dorale, J.A., 2001. A high-resolution absolute-dated late pleistocene monsoon record from Hulu Cave, China. Science 294, 2345–2348.
Wu, G.X., Chou, J.F., Liu, Y.M., Zhang, Q.Y., Sun, S.Q., 2003. Review and prospect of the study on the subtropical anticyclone. Chinese J. Atmos. Sci. 27, 503–517 (in Chinese with English summary).
Ying, M., Sun, S.Q., 2000. A study on the response of subtropical high over the western Pacific on the SST anomaly. Chinese J. Atmos. Sci. 24, 193–206 (in Chinese with English summary).
Yuan, D.X., Cheng, H., Edwards, R.L., Dykoski, C.A., Kelly, M.J., Zhang, M.L., Qing, J.M., Lin, Y.S., Wang, Y.J., Wu, J.Y., Dorale, J.A., An, Z.S., Cai, Y.J., 2004. Timing, duration, and transitions of the last interglacial Asian monsoon. Science 304, 575–578.
Zhong, W., 1998. The younger Dryas cooling event reflected by carbonate isotopic data from Bosten Lake sediment during late deglaciation. Mar. Geol. Quat. Geol. 18, 87–94.
Zhong, W., Xue, J.B., Cao, J.X., Zheng, Y.M., Ma, Q.H., Ouyang, J., Cai, Y., Zeng, Z.G., Liu, W., 2010. Bulk organic carbon isotopic record of lacustrine sediments in Dahu Swamp, eastern Nanling Mountains in South China: implication for catchment environmental and climatic changes in the last 16 000 years. J. Asian Earth Sci. 38, 162–169.
Zhou, W.J., Donahue, D.J., Porter, S.C., Jull, T.A., Li, X.Q., Stuiver, M., An, Z.S., Matsumoto, E., Dong, G.R., 1996. Variability of monsoon climate in East Asia at the end of the last glaciation. Quat. Res. 46, 219–229.